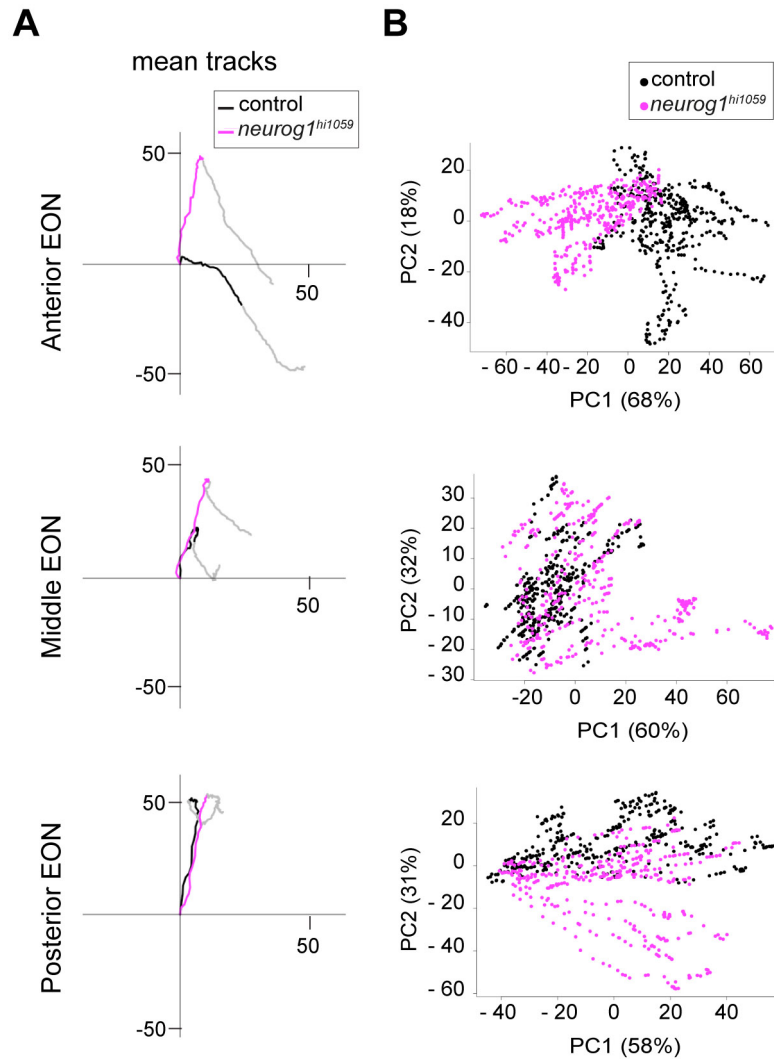


**Fig. S1.** *neurog1* mutant embryos display specific defects in olfactory development.

(**A**) Schematic representation of the relative antero-posterior length calculation. Lengths are normalised relative to the 12 hpf antero-posterior length. (**B**) Graph showing normalised antero-posterior length of the developing olfactory cups in control (Black) and *neurog1*<sup>hi1059</sup> mutant embryos (Magenta) over time. The mean  $\pm$  s.e.m of 3 embryos/6 cups are represented per condition.



**Fig. S2.** Anterior EON population tracks are specifically affected in *neurog1* mutated embryos.

**(A)** Mean tracks for anterior, middle and posterior EON of control (Black) or *neurog1<sup>hi1059</sup>* mutant (Magenta) embryos. Means are from 12 tracks (2 cells each from the left and right of 3 embryos) for each region. The origin of the tracks has been arbitrarily set to the intersection of the X/Y axis and the early (coloured) and late (Grey) phases of migration have been highlighted. **(B)** Pairwise principal component analysis scatterplots of morphogenetic parameters extracted from the datasets presented in **(A)**. Whereas for anterior PC1 and PC2 respectively correspond to the antero-posterior and medio-lateral axes, for middle and posterior PC1 and PC2 represent the antero-posterior and superficial-deep axes.

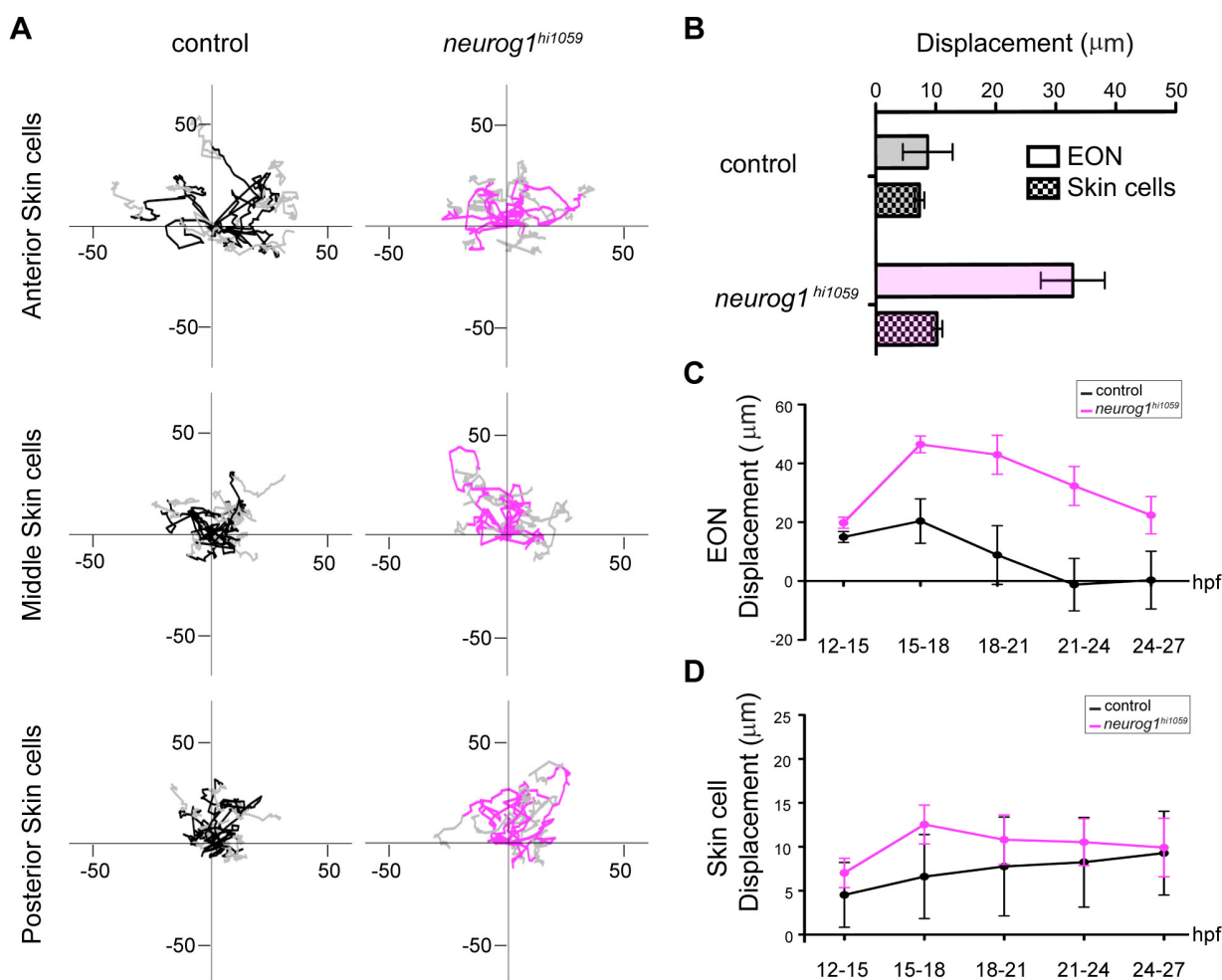


**Fig. S3.** Morphogenetic movements of skin cells in *neurog1<sup>hi1059</sup>* mutant embryos.

Tracks showing migration of skin cells in control (Black) or *neurog1<sup>hi1059</sup>* mutant (Magenta) embryos. 12 tracks are represented for cells overlying the anterior, middle and posterior domains of the developing cup. The origin of the tracks has been arbitrarily set to the intersection of the X/Y axis and the early (coloured) and late (Grey) phases of migration have been highlighted. Morphogenetic movements of individual skin cells showed no obvious differences in control versus *neurog1* mutants. **(B)** Histogram showing the sum of the displacement of EON (empty) and skin cells (checked) of control (Black) and *neurog1<sup>hi1059</sup>* mutant embryos (Magenta) along the antero-posterior axis during olfactory cup development. The mean  $\pm$  s.e.m of 12 cells are represented per condition. **(C)** Graph showing the sum of the displacement along the antero-posterior axis of control (Black) or *neurog1<sup>hi1059</sup>* mutant (Magenta) EON during five indicated time periods. The mean  $\pm$  s.e.m of 36 cells are represented (12 cells per embryo and 3 embryos per genotype) per condition. **(D)** Graph showing the sum of the displacement along the antero-posterior axis of control (Black) or *neurog1<sup>hi1059</sup>* mutant (Magenta) skin cells during five indicated time periods. The mean  $\pm$  s.e.m of 36 cells are represented (12 cells per embryo and 3 embryos per genotype) per condition.

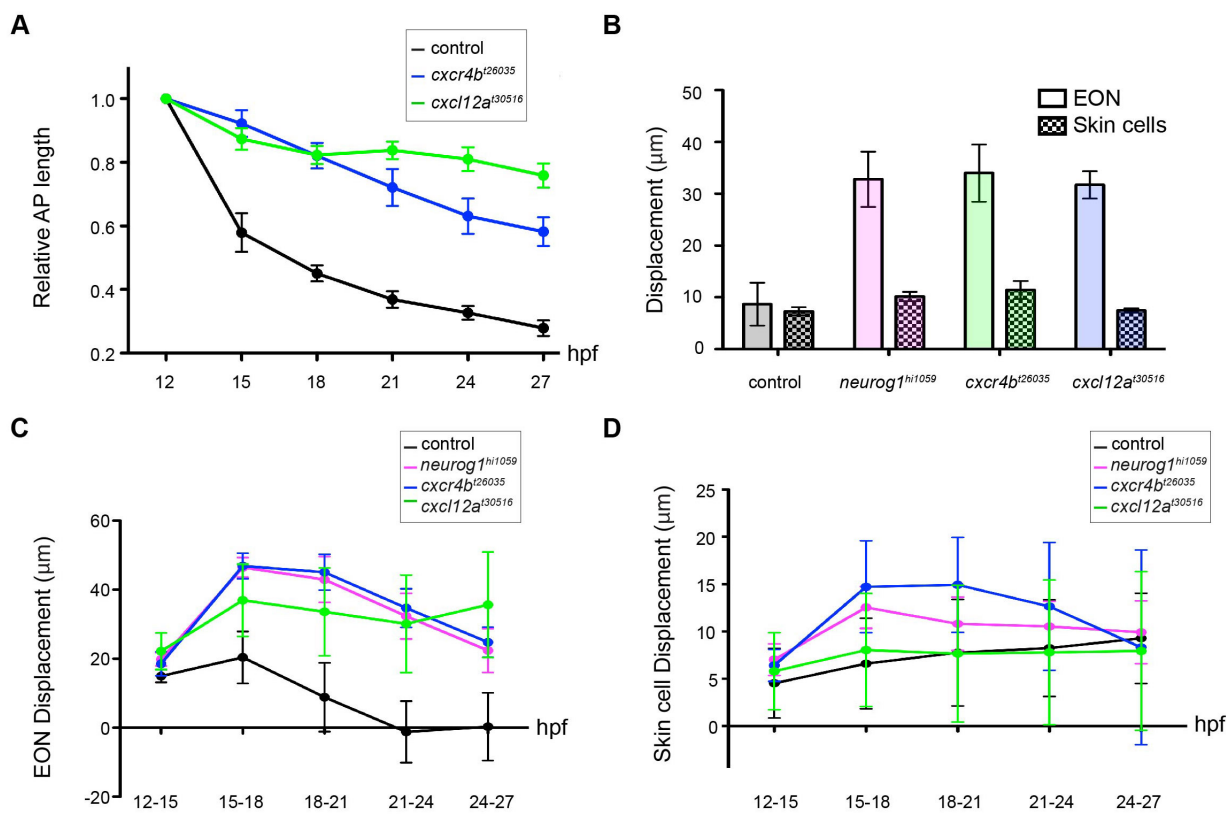


**Fig. S4.** Morphogenetic movements of EON are globally affected in *cxcr4b*<sup>t26035</sup> and *cxcl12a*<sup>t30516</sup> mutant embryos.

(A) Graph showing normalised antero-posterior length of the developing olfactory cup in control (Black) and *cxcr4b*<sup>t26035</sup> (Blue) and *cxcl12a*<sup>t30516</sup> (Green) mutants over time. The mean  $\pm$  s.e.m of 3 embryos/6 cups are represented per condition. (B) Histogram showing the sum of the displacement of EON (empty) and skin cells (checked) for control (Black), *neurog1*<sup>hi1059</sup> (Magenta) *cxcr4b*<sup>t26035</sup> (Blue) and *cxcl12a*<sup>t30516</sup> (Green) mutants along the antero-posterior axis during olfactory cup development. The mean  $\pm$  s.e.m of 12 cells are represented per condition. (C) Graph showing the sum of the displacement along the antero-posterior axis of control (Black), *neurog1*<sup>hi1059</sup> (Magenta) *cxcr4b*<sup>t26035</sup> (Blue) and *cxcl12a*<sup>t30516</sup> (Green) EON during five indicated time periods. The mean  $\pm$  s.e.m of 36 cells are represented (12 tracks per embryo and 3 embryos per genotype) per condition. (D) Graph showing the sum of the displacement along the antero-posterior axis of control (Black), *neurog1*<sup>hi1059</sup> (Magenta) *cxcr4b*<sup>t26035</sup> (Blue) and *cxcl12a*<sup>t30516</sup> (Green) skin cells during five indicated time periods. The mean  $\pm$  s.e.m of 36 cells are represented (12 tracks per embryo and 3 embryos per genotype) per condition.

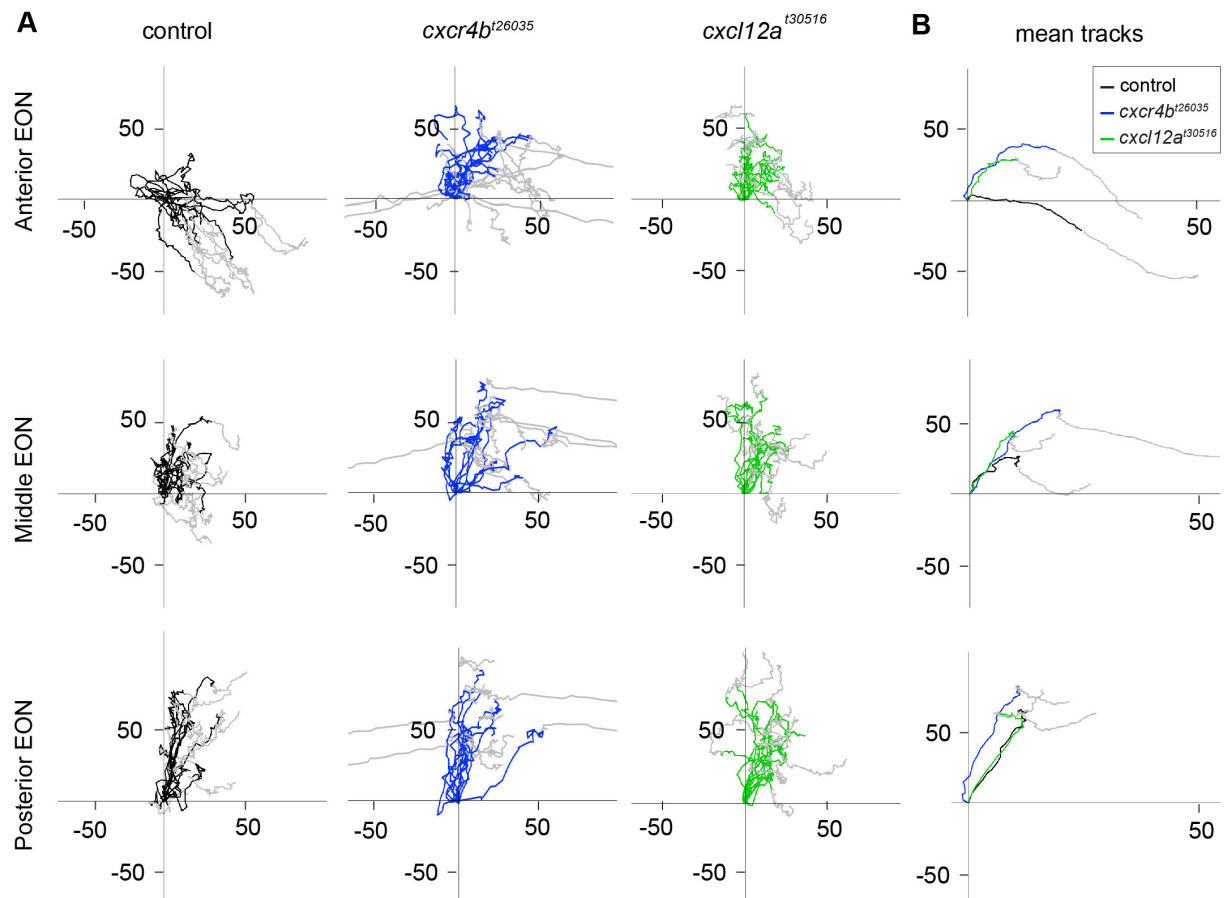


**Fig. S5.** Morphogenetic parameters in *cxcr4b*<sup>t26035</sup> and *cxcl12a*<sup>t30516</sup> mutant embryos.

(A) Tracks showing migration of EON of control (Black), *cxcr4b*<sup>t26035</sup> (Blue) and *cxcl12a*<sup>t30516</sup> (Green) embryos. 12 tracks are represented (2 cells each from the left and right of 3 embryos) for each of the anterior, middle and posterior domains of the developing cup. The origin of the tracks has been arbitrarily set to the intersection of the X/Y axis and the early (coloured) and late (Grey) phases of migration have been highlighted. (B) Mean tracks for anterior EON of control (Black), *cxcr4b*<sup>t26035</sup> (Blue) and *cxcl12a*<sup>t30516</sup> (Green) embryos.

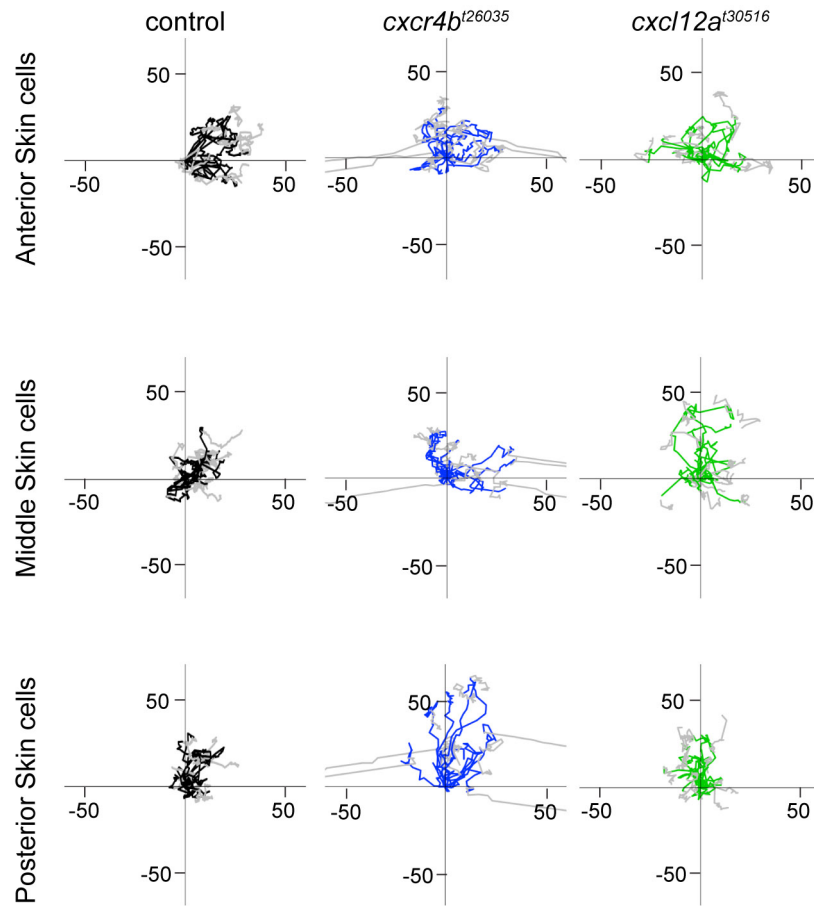


**Fig. S6.** Morphogenetic movements of skin cells in *cxcr4b*<sup>t26035</sup> and *cxcl12a*<sup>t30516</sup> embryos.

Tracks showing migration of skin cells of control (Black), *cxcr4b*<sup>t26035</sup> (Blue) and *cxcl12a*<sup>t30516</sup> (Green) embryos. 12 tracks are represented for cells overlying the anterior, middle and posterior domains of the developing cup. The origin of the tracks has been arbitrarily set to the intersection of the X/Y axis and the early (coloured) and late (Grey) phases of migration have been highlighted. Morphogenetic movements of individual skin cells showed no obvious differences in control versus *cxcr4b*<sup>t26035</sup> or *cxcl12a*<sup>t30516</sup> embryos.

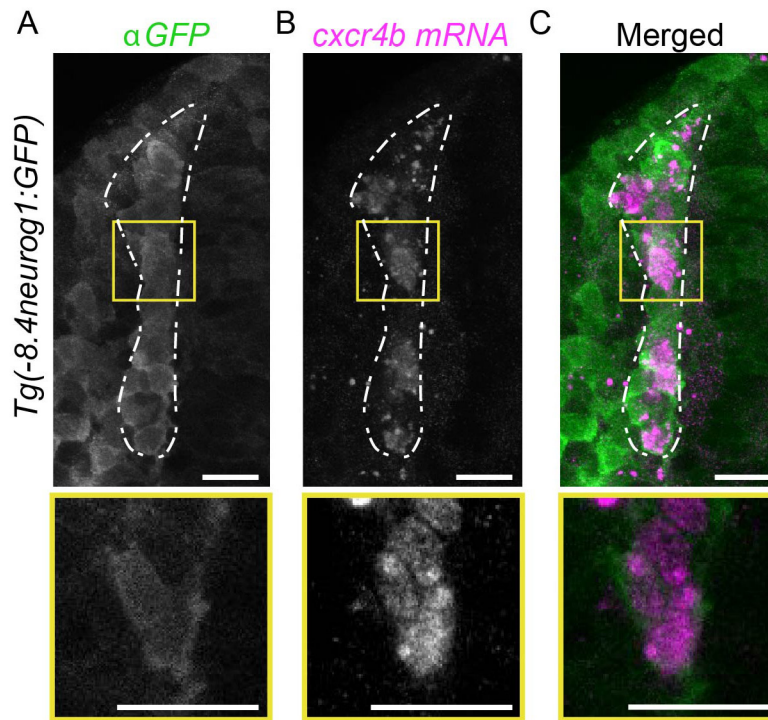


**Fig. S7.** The expression of *neurog1* and *cxcr4b* overlap in the developing olfactory placode.

(A-C) Confocal projections of olfactory placodes showing co-expression of GFP (green) from the *Tg(8.4neurog1:GFP)* transgene with *cxcr4b* transcripts (magenta) at 14 hpf. The position of the magnified regions in the second row of panels, which contain single confocal sections, is indicated with yellow squares. Scale bars represent 20 $\mu$ m.

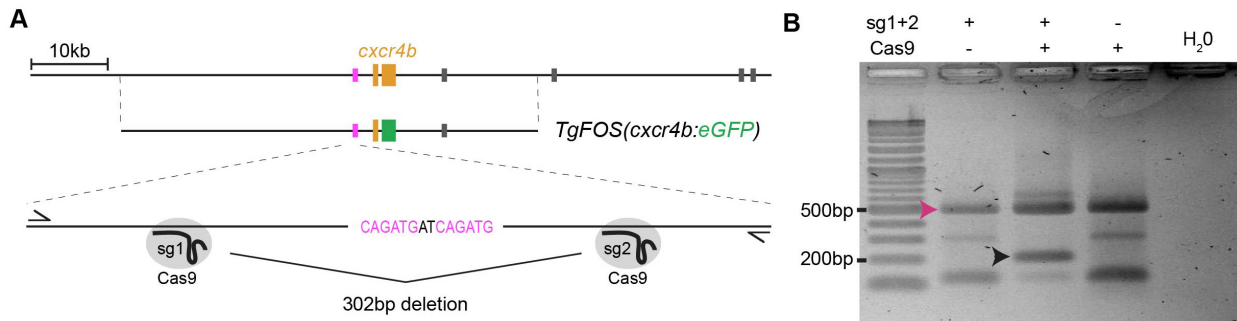
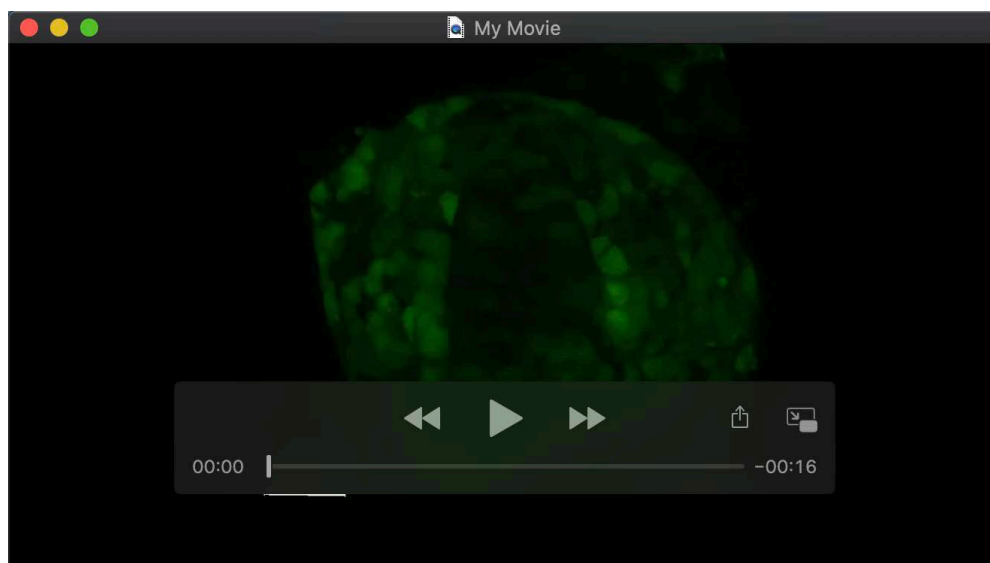


**Fig. S8.** Crispr-Cas9 deletion of the Neurog1-regulated CRM upstream of the *cxcr4b* locus.

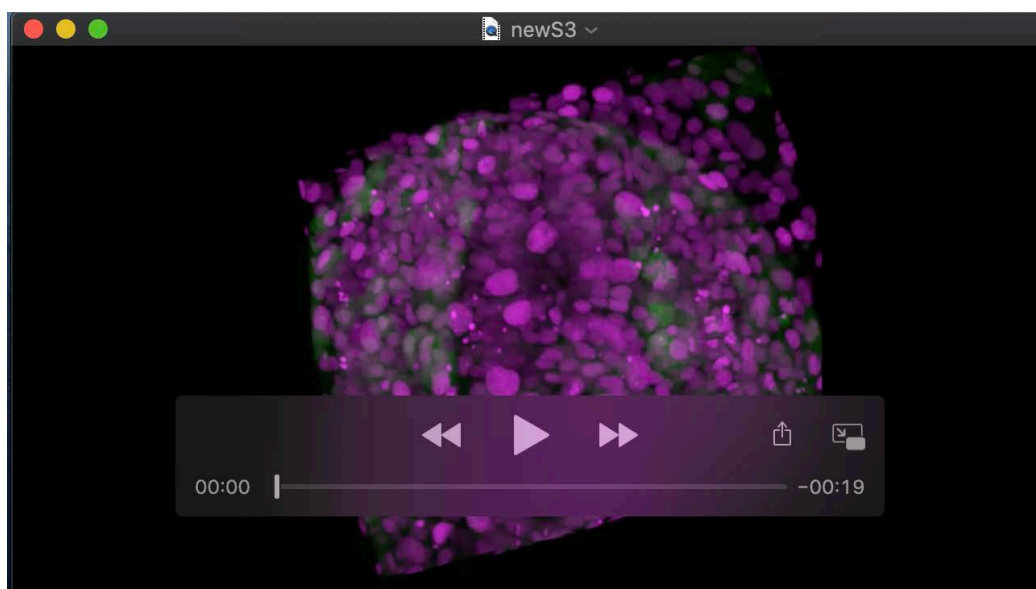
(A) Schematic representation of the *cxcr4b* locus indicating the position of exons of the *cxcr4b* gene (orange) and E-box clusters, which are color-coded depending on the nature of the E-box sequences. The position of the genomic sequences found in the *TgFOS(cxcr4b:eGFP)* transgene and a schematic representation of the PCR fragment used to genotype potential deletions with the sequence of the E-box cluster are also shown. (B) Ethidium bromide stained agarose gel showing the results of PCR genotyping for the induction of deletions of the CAGATG E-box cluster. The magenta arrowhead shows the 500bp control band. A 200bp band appears (black arrowhead) when the sgRNA pair is injected with Cas9 but not when the sgRNA pair or Cas9 is injected alone (bp, base pair).





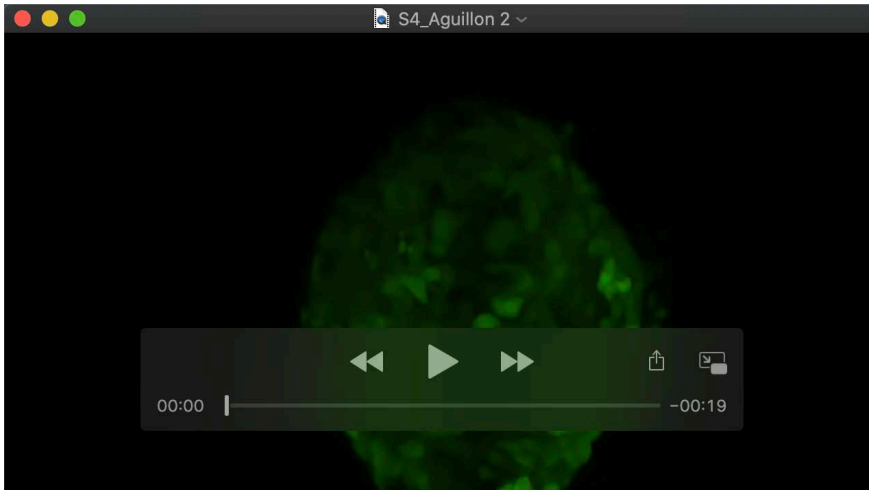
**Movie 1.** Time-lapse imaging reveals a convergence migration of EON towards the centre of the future olfactory cup.

Movie showing an acquisition series of *Tg(-8.4neurog1:gfp)* labelled EON in a control embryo. The movie shows the entire acquisition from 12 to 27 hpf with frames every 7 min. The Movie has been annotated at 12, 18 and 27 hpf to indicate the preplacodal ectoderm (PPE), olfactory placode (OP), olfactory epithelium (OE), Anterior Neural Plate and Telencephalon.



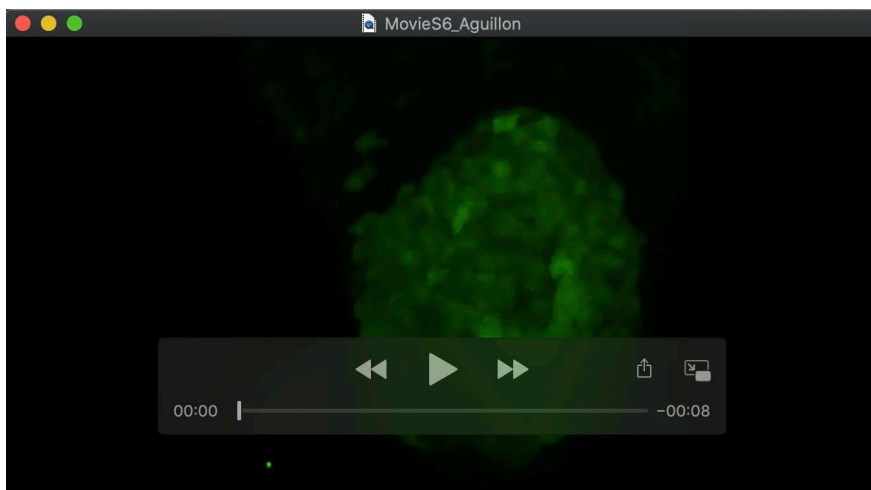
**Movie 2.** Tracking EON behaviour at single-cell resolution.

Behaviour of EON located in the anterior, middle and posterior thirds of the *neurog1:GFP+* population was established by manually tracking H2B-RFP positive nuclei. The movie is divided into 6 parts representing: the acquisition showing *neurog1:GFP+* cells (Green) and their nuclei (Magenta), tracking of anterior, middle and posterior EON cells, all tracking combined and a still image showing the tracks from anterior, middle and posterior cells.



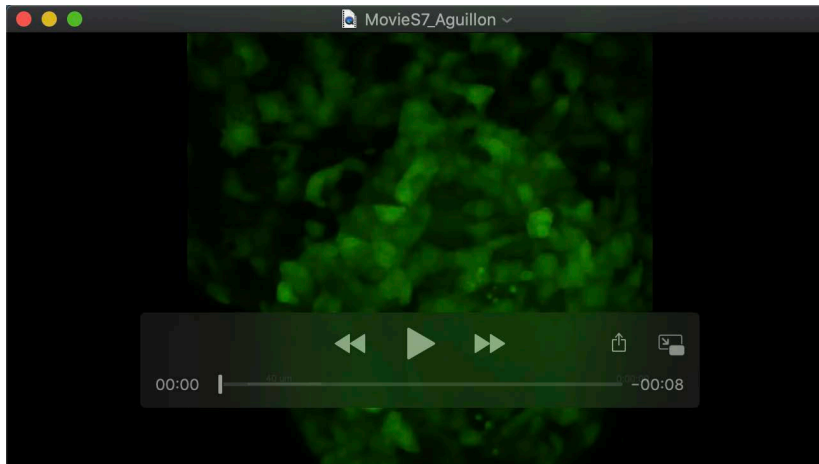
**Movie 3.** Tracking EON behaviour at single-cell resolution in *neurog1*<sup>hi1059</sup> mutant embryo.

The movie is divided into 6 parts representing: the acquisition showing neurog1:GFP cells, tracking of anterior, middle and posterior EON cells, all tracking combined and a still image showing the tracks from anterior, middle and posterior cells; the early phase of migration that is affected in the mutant is highlighted (Magenta).



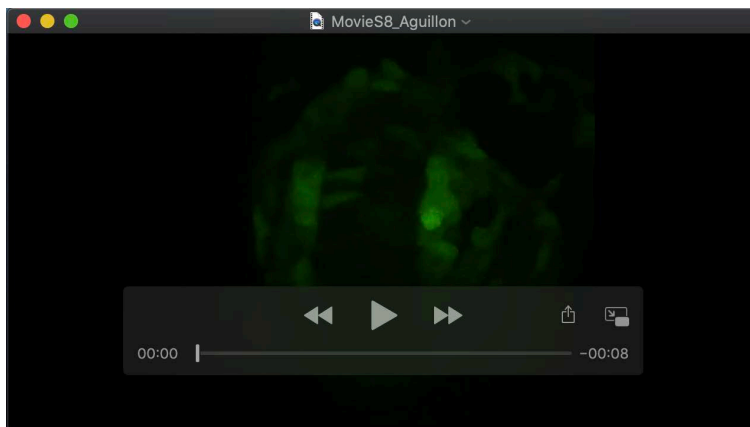
**Movie 4.** Tracking EON behaviour at single-cell resolution in *cxcr4b*<sup>t26035</sup> mutant embryo.

The movie is divided into 3 parts representing: the acquisition showing neurog1:GFP cells, tracking of a pair of anterior EON cells and a still showing the anterior tracks; the early phase of migration that is affected in the mutant is highlighted (Blue).



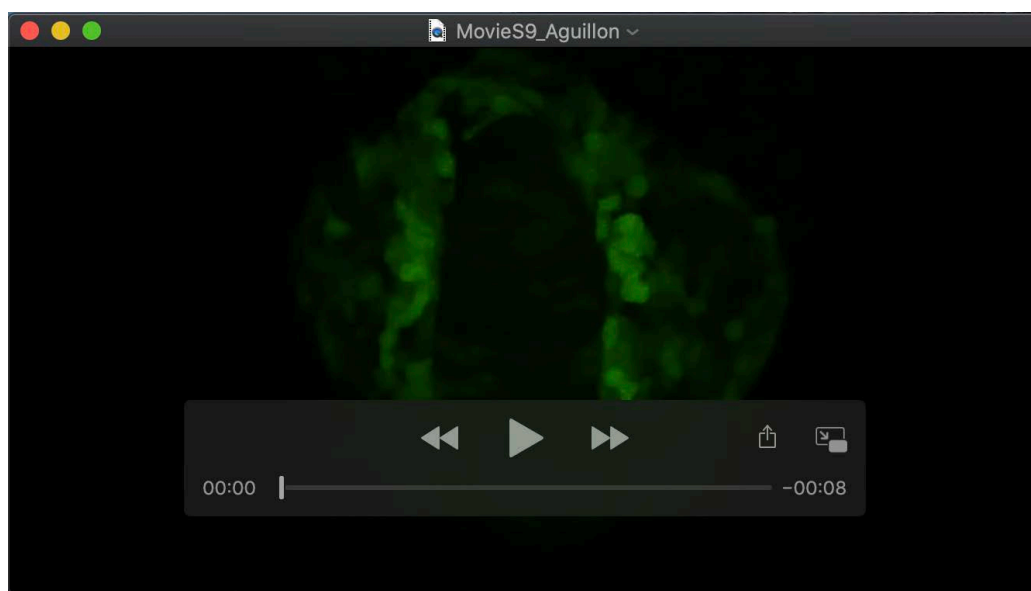
**Movie 5.** Tracking EON behaviour at single-cell resolution in *cxcl12a*<sup>t30516</sup> mutant embryo.

The movie is divided into 3 parts representing: the acquisition showing neurog1:GFP cells, tracking of a pair of anterior EON cells and a still showing the anterior tracks; the early phase of migration that is affected in the mutant is highlighted (Green).



**Movie 6.** Re-expressing Cxcr4b in *neurog1*<sup>hi1059</sup> mutant embryo rescues anterior EON behaviour.

The movie is divided into 3 parts representing: the acquisition showing neurog1:GFP cells, tracking of an anterior EON cell and a still showing the anterior track; the early phase of migration is highlighted (Cyan).



**Movie 7.** Rescue transgene expression does not affect anterior EON behaviour in a control context.

The movie is divided into 3 parts representing: the acquisition showing neurog1:GFP cells, tracking of an anterior EON cell and a still showing the anterior track; the early phase of migration is highlighted (Light Blue).